# Nuclear modification of light flavour and strangeness at LHC energies with ALICE



IOP Conf. Series: Journal of Physics: Conf. Series **878** (2017) 012006 doi:10.1088/1742-6596/878/1/012006

# Nuclear modification of light flavour and strangeness at LHC energies with ALICE

**Ramona Lea for the ALICE Collaboration**

University and INFN Trieste, Via Valerio 2, 34127 Trieste, Italy

E-mail: ramona.lea@cern.ch

**Abstract.** Thanks to its unique particle identification capabilities the ALICE detector is able to identify light-flavour, strange and multi-strange hadrons, including $\pi$, K, p, $K^0_S$, $\Lambda$, $\Xi$ and $\Omega$, over a wide range of transverse momentum, from pp and p-Pb interactions up to central Pb–Pb collisions. The latest results on the nuclear modification factor, $R_{\rm AA}$, as a function of the Pb–Pb collision centrality, is shown for various particle specie at $\sqrt{s_{\rm NN}} = 2.76$ TeV centre-of-mass energy. For each particle specie, the $R_{\rm AA}$ is compared with the nuclear modification factors $R_{\rm pA}$ in p-Pb collisions to asses the presence of hot nuclear matter effects affecting the high-$p_{\rm T}$ particle production in Pb–Pb collisions. The results on the $R_{\rm AA}$ of charged hadrons at $\sqrt{s_{\rm NN}} = 5.02$ TeV, the highest energy ever reached in the laboratory for heavy-ion collisions, is also shown.

## 1. Introduction

One of the main goals of ultra relativistic heavy-ion collisions is the study of strongly interacting matter where the formation of the Quark-Gluon Plasma (QGP), a deconfined state of quarks and gluons, is expected [1]. Hard partons that propagate through this matter are predicted to loose energy via (multiple) scattering and gluon radiation. As a result, transverse momentum ($p_{\rm T}$) spectra of final state hadrons and jets will be modified with respect to what is expected from a simple superposition of incoherent proton-proton collisions. This change, quantified by the nuclear modification factor, $R_{\rm AA}$, is used to study parton energy-loss mechanisms and medium properties. Disentangling energy-loss signatures from initial state nuclear effects which may also modify $p_{\rm T}$ spectra, requires a comparison of $R_{\rm AA}$ to $R_{\rm pA}$, the nuclear modification factor for proton-nucleus collisions. In this paper, an overview of ALICE results on the nuclear modification factor for identified hadrons at $\sqrt{s_{\rm NN}} = 2.76$ TeV and charged particles at $\sqrt{s_{\rm NN}} = 5.02$ TeV are presented.

A full description of the ALICE detector and its performance can be found in [2]. The ALICE sub-detectors that played an essential role for the analysis presented here are the V0 detectors [3] – covering the pseudorapidity ranges $2.8 < \eta < 5.1$ (V0-A) and $-3.7 < \eta < -1.7$ (V0-C) – the Inner Tracking System (ITS) [4] – composed of six cylindrical layers of silicon detectors with radii between 3.9 and 43 cm from the beam axis – the Time Projection Chamber (TPC) [5], which is the main tracking detector, and the Time-Of-Flight (TOF) detector [6]. At high momenta ($> 1$ GeV/$c$) identification is complemented by a small acceptance ring imaging Cherenkov detector, the HMPID [2].

The nuclear modification factor $R_{\rm AA}$ is defined as:

$$R_{AA} = \frac{1}{\langle T_{\rm AA}\rangle}\frac{{\rm d}N_{\rm AA}/{\rm d}p_{\rm T}}{{\rm d}\sigma_{pp}/{\rm d}p_{\rm T}} \quad (1)$$

where $N_{\rm AA}$ and $\sigma_{pp}$ represent the yield in nucleus-nucleus collisions and the cross section in pp collisions, respectively. $\langle T_{\rm AA}\rangle = \langle {\rm N}_{\rm coll}\rangle$ / $\sigma_{inel}^{NN}$ is the nuclear overlap function, which corresponds to the ratio of the number of binary nucleon-nucleon collisions $\langle {\rm N}_{\rm coll}\rangle$ estimated with a Glauber model [7] and the inelastic nucleon-nucleon cross section $\sigma_{inel}^{NN}$. If the Pb–Pb collisions are a simple superpositions of elementary nucleon-nucleon collisions, the $R_{\rm AA}$ is expected to be equal to unity, while $R_{\rm AA}< 1$ indicates a suppression of charged-particle production compared to binary-collision scaling.

## 2. $R_{\rm AA}$ of identified hadrons at $\sqrt{s_{\rm NN}} = 2.76$ TeV

ALICE employs several complementaries particle identification techniques. Specifically, charged pions, kaons and protons at high transverse momentum are identified via the specific ionization ${\rm d}E/{\rm d}x$ measured in the TPC. For $p_{\rm T} < 4$ GeV/$c$, the combined PID of the HMPID, the TOF detector and ${\rm d}E/{\rm d}x$ in the ITS and TPC are used. Neutral strange and multi-strange particles ($\rm K^0_S$, $\Lambda$, $\overline{\Lambda}$) and multi-strange baryons ($\Xi$ and $\Omega$) are reconstructed via topological selection criteria and invariant-mass analysis of their characteristic weak decays. Specifically, tracks reconstructed by the TPC and the ITS are combined to select candidates satisfying a set of geometrical criteria. In addition, particle identification of the decay products is performed via a selection based on the specific energy loss in the TPC. Particle yields as a function of $p_{\rm T}$ are determined in various centrality intervals using an invariant mass analysis. Acceptance and efficiency corrections are calculated using Monte Carlo simulations. For more details, refer to [8–10].

### *2.1. Results*

The transverse momentum spectra of charged pions, kaons and protons as well as $\rm K^0_S$ and hyperons in Pb–Pb collisions at $\sqrt{s_{\rm NN}} = 2.76$ TeV have been published in [8,11,12]. At low $p_{\rm T}$ a flattening of the spectra is observed, which is more pronounced for central collisions and heavier particles. The mass dependence of this effect is characteristic of radial flow during the collective expansion of the fireball. In Figure 1 the $R_{\rm AA}$ as a function of $p_{\rm T}$ for multi-strange baryons is compared to the one for lighter hadrons for two different centrality intervals, 0-10% (left) and 60-80% (right). At high $p_{\rm T}$ the $R_{\rm AA}$ of pions, kaons, protons and $\Xi$ baryons is significantly smaller than unity. The suppression is stronger for the 10% most central collisions (left panel) than for peripheral collisions (60-80% central, right panel). At $p_{\rm T} > 10$ GeV/$c$, the $R_{\rm AA}$ of $\pi$, K, and p is similar [11]. The absence of a specie dependence may indicate vacuum-like parton fragmentation for the partons that will originate high-$p_{\rm T}$ hadrons in the final state. Differences at low $p_{\rm T}$ ($p_{\rm T} \leq 6$ GeV/$c$) may be attributed to the mass-dependent flow effects. The nuclear modification factor for $\Xi$ is similar to the one for p, while $R_{\rm AA}$ for $\Omega$ shows a pronounced difference with respect to $\Xi$ and exceeds unity, which might be the result of larger strangeness enhancement compared to $\Xi$ [8]. In peripheral collisions the difference between the $R_{\rm AA}$ of $\Omega$ and $\Xi$ is strongly reduced, as can be observed in the right panel of Figure 1. In Figure 2 the $R_{\rm pPb}$ as a function of $p_{\rm T}$ in minimum-bias p–Pb collisions at $\sqrt{s_{\rm NN}} = 5.02$ TeV is shown for $\pi$, K, p, $\Xi$ and $\Omega$. In this case, there is no suppression for $\pi$, K and p at high $p_{\rm T}(> 6$ GeV/$c$) [13], as found for unidentified particles [14]. This observation leads to the conclusion that the observed suppression in Pb–Pb collisions is a hot matter effect. Finally, in the so-called Cronin region ($2 < p_{\rm T} < 6$ GeV/$c$) an increase of the $R_{\rm pPb}$ with the mass and the strangeness content of the particles is visible.

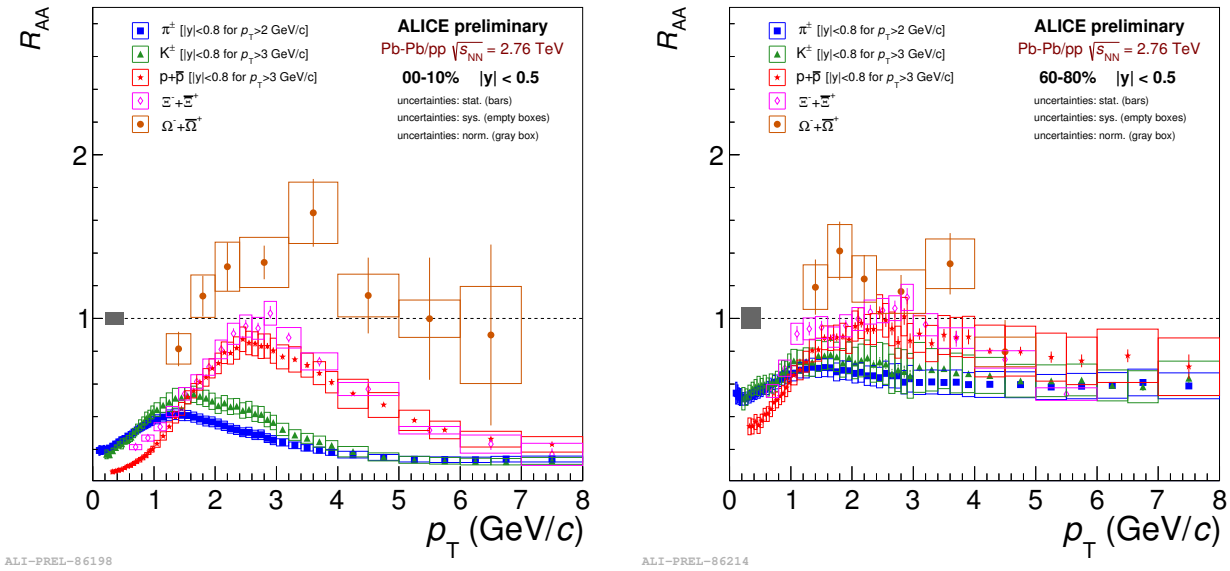


Figure 1: Nuclear modification factor $R_{\mathrm{AA}}$ for charged $\pi$, K, p, $\Xi$ and $\Omega$ particles in 0-10% central (left) and 60-80% central (right) Pb–Pb collisions at $\sqrt{s_{\mathrm{NN}}} = 2.76$ TeV. Bars represents statistical uncertainties, open boxes systematic uncertainties while gray boxes are normalization uncertainties.

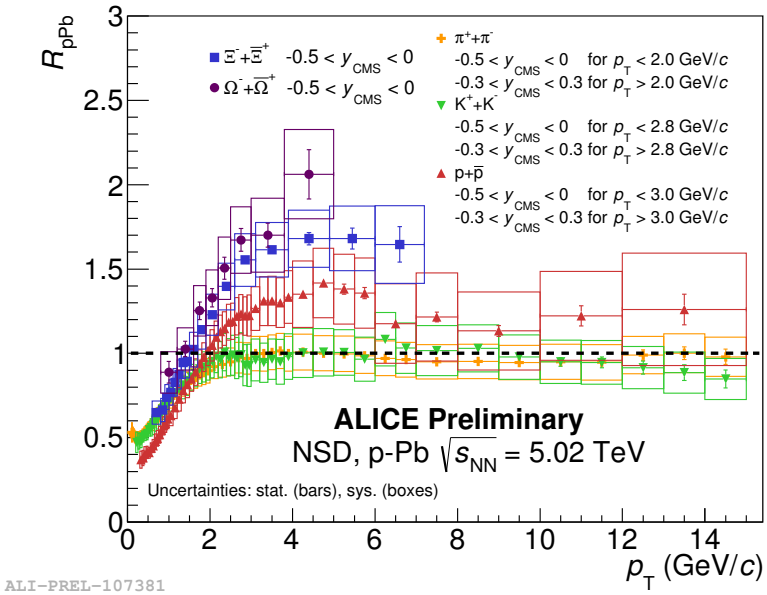


Figure 2: $R_{\mathrm{pPb}}$ as a function of $p_{\mathrm{T}}$ in minimum-bias p–Pb collisions of $\pi$, K, p, $\Xi$ and $\Omega$. Bars represents statistical uncertainties, while open boxes systematic uncertainties.

## 3. $R_{\rm AA}$ of charged hadrons at $\sqrt{s_{\rm NN}} = 5.02$ TeV

The results presented in this section are based on the analysis of $25 \times 10^6$ pp collisions and $3.3 \times 10^6$ Pb–Pb collisions at $\sqrt{s_{\rm NN}} = 5.02$ TeV collected by ALICE during 2015, which represent approximately 25% and 3% of the full collected statistics, respectively. Events are triggered using the V0A and V0C detectors, which in Pb–Pb collisions are also used to determine the centrality of the collision [15]. For the measurement of the charged particle spectra, only primary particles are selected. Primaries are defined as all the prompt charged particles produced in the collisions including all decay products, except charged particles from weak decay of light flavour hadrons.

All the corrections applied to the data are calculated using PYTHIA8 [16] Monte Carlo simulations for pp and HIJING [17] for Pb–Pb collisions where the particle transport in the ALICE detector is simulated via GEANT3 [18]. To account for the differences in particle composition between event generators and data, the charged-particle reconstruction efficiency was calculated from particle-dependent efficiencies weighted by the relative particle abundances measured in pp collisions at 7 TeV and Pb–Pb collisions at 2.76 TeV. The correction for contamination by secondary particles produced from weak decay or secondary interaction is important only at low $p_{\rm T}$ ($\sim 10\%$), while the correction for $p_{\rm T}$ resolution is important at high $p_{\rm T}$ ($\sim 2\%$).

### *3.1. Results*

The transverse momentum distributions have been measured for pp and Pb–Pb collisions at the same energy per colliding nucleon pair $\sqrt{s_{\rm NN}} = 5.02$ TeV. The left panel of Figure 3 shows the $p_{\rm T}$ spectrum of charged particles for pp collisions at $\sqrt{s}$= 5.02 TeV in the $p_{\rm T}$ interval $0.15 \leq p_{\rm T} \leq 40$ GeV/$c$ and $|\eta| < 0.8$. The measurement is compared to Monte Carlo calculations performed with PYTHIA8 (Monash-2013 tune) [16] and EPOS LHC [19]. Both models describe the data reasonably well at intermediate $p_{\rm T}$, but both overestimate the production at low and high $p_{\rm T}$ by a similar amount ($\sim 20\%$). The Pb–Pb transverse momentum distributions for six centralities are shown on the right panel of Figure 3. On the same panel the pp references scaled with the nuclear overlap function $\langle T_{\rm AA} \rangle$ are shown as dashed lines.

The nuclear modification factor can be calculated as the ratio of the two distributions. The $R_{\rm AA}$ for six different centralities as a function of $p_{\rm T}$ is shown in Figure 4. The solid symbols correspond to the measurement at $\sqrt{s_{\rm NN}} = 5.02$ TeV while the open symbols represent the published data at $\sqrt{s_{\rm NN}} = 2.76$ TeV [20]. For the six centrality intervals, the measurements for both energies show a similar behavior within systematic uncertainties. In central collisions (0-5%) a strong suppression is observed, with a minimum at $p_{\rm T} \sim 7$ GeV/$c$ and a significant rise for $p_{\rm T} > 7$ GeV/$c$. For peripheral collisions (60-80%) $R_{\rm AA}$ exhibits a moderate suppression ($\sim 0.7$).

Figure 5 shows the comparison of the measured $R_{\rm AA}$ at $\sqrt{s_{\rm NN}} = 5.02$ TeV with different theoretical models. On the left panel the measurement in the 0-5% centrality interval is compared with the model proposed by Djordjevic at al. [21] (long dashed lines) and by Majumder et al. [22] (dashed lines). Djordjevic et al. model uses a dynamical energy loss formalism and takes into account interactions of the probe with the medium. Both the radiative and the collisional energy loss mechanisms are implemented in the model. Additionally, the formalism also takes into account finite magnetic mass and running coupling. Majumder et al. model is based on a higher twist (HT) radiative energy loss calculation and uses a viscous hydrodynamical evolution of the system. The model parameters are adjusted from soft hadron yield and elliptic flow. The two models succeed in describing the $R_{\rm AA}$ measurements at high $p_{\rm T}$. On the right panel of Figure 5 the measurement in the 0-10% centrality interval is compared with the predictions from the model of Vitev et al. [23], which is based on the soft-collinear effective theory (SCET) [24], an effective theory of QCD for jet physics. Also in this case the model describes the data within the model uncertainties.

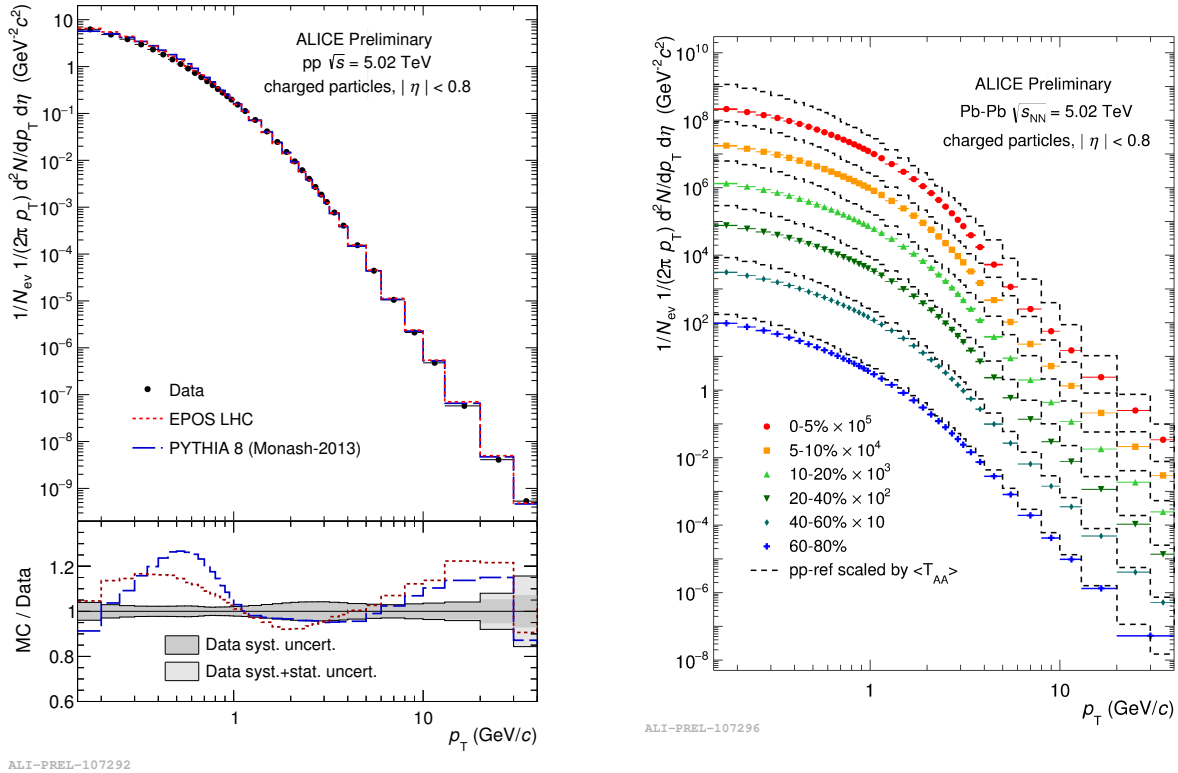


Figure 3: Left: Transverse momentum distribution of charged particles for pp collisions at $\sqrt{s}$=5.02 TeV, compared to PYTHIA8 and EPOS calculations [16, 19]. Right: Transverse momentum distribution of charged particles for Pb–Pb collisions at $\sqrt{s_{\rm NN}}$ = 5.02 TeV for six different centrality classes. The dashed lines represent the measured pp collisions scaled by $\langle T_{\rm AA}\rangle$.

## 4. Conclusions

The production of charged pions, kaons and protons, neutral strange mesons and hyperons was measured with the ALICE detector in pp, p–Pb and Pb–Pb collisions. In central Pb–Pb collisions, $R_{\rm AA}$ of light hadrons at high $p_{\rm T}$ is smaller than unity, indicating a suppression attributed to parton energy loss. The nuclear modification factor of charged pions, kaons and protons is similar for $p_{\rm T} > 10$ GeV/$c$, hinting at vacuum-like fragmentation of the leading parton. The $R_{\rm AA}$ of $\Xi$ is consistent with the $R_{\rm AA}$ of p for $p_{\rm T}$ larger than 6 GeV/$c$, whereas the $R_{\rm AA}$ of $\Omega$ is significantly higher. The difference between the $R_{\rm AA}$ of $\Omega$ and $\Xi$ is much less pronounced in peripheral collisions. The absence of a suppression at high $p_{\rm T}$ in $R_{\rm pPb}$ indicates that the suppression in $R_{\rm AA}$ is due to hot nuclear matter effect.

The nuclear modification factor of unidentified charged particles in Pb–Pb collisions at $\sqrt{s_{\rm NN}} = 5.02$ TeV was measured and it was found to be similar to the measurement at 2.76 TeV. A maximal suppression was observed around 6-7 GeV/$c$ for the most central collisions (0-5%) which becomes smaller as centrality decreases. The $R_{\rm AA}$ was compared with three models and they succeed in describing the general features of the measurement for a transverse momentum $p_{\rm T}$ larger than 5 GeV/$c$.

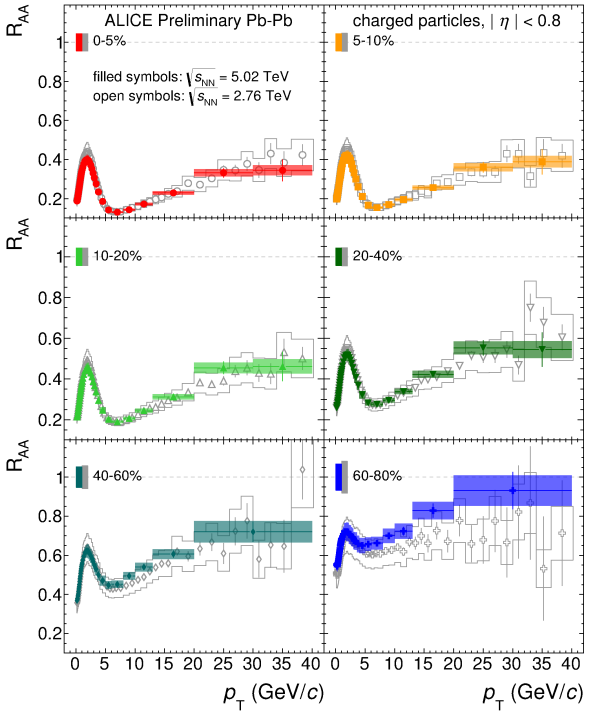


Figure 4: The nuclear modification factor ($R_{\mathrm{AA}}$) as a function of $p_{\mathrm{T}}$ for six centrality intervals. Filled symbols represent the measurements at $\sqrt{s_{\mathrm{NN}}} = 5.02$ TeV, while empty symbols corresponds to the $R_{\mathrm{AA}}$ at $\sqrt{s_{\mathrm{NN}}} = 2.76$ TeV [20]. The normalization uncertainty is shown for both energies as a box around unity.

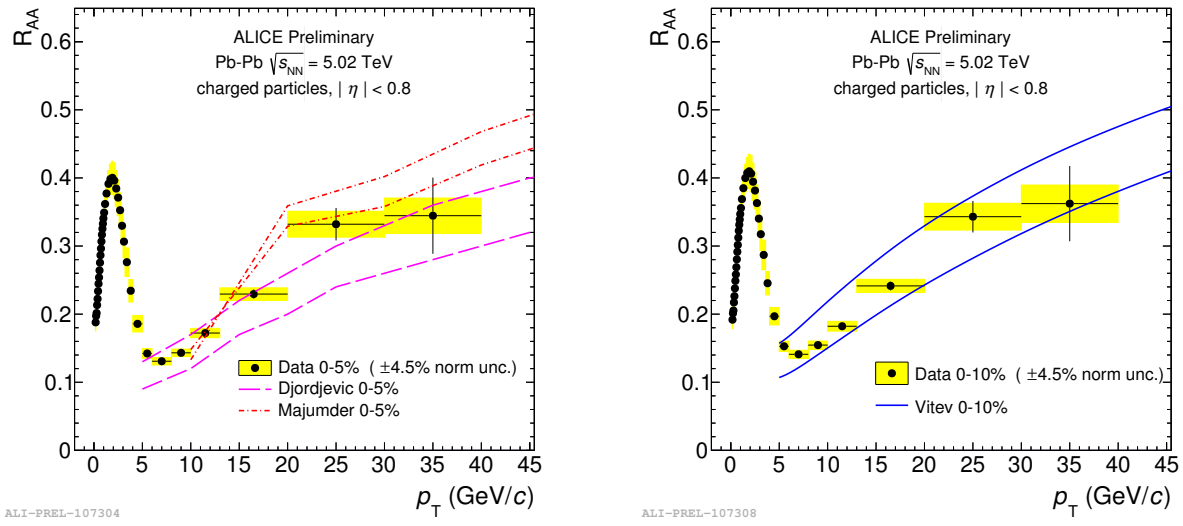


Figure 5: The nuclear modification factor measured at $\sqrt{s_{\mathrm{NN}}} = 5.02$ TeV for 0-5% (left) and 0-10% (right) centrality intervals compared to different theoretical models calculations [21–23].

## References

[1] H. Stoecker and W. Greiner, Phys. Rept. **137** (1986) 277.
[2] B. B. Abelev *et al.* [ALICE Collaboration], Int. J. Mod. Phys. A **29** (2014) 1430044
[3] E. Abbas *et al.* [ALICE Collaboration], JINST **8** (2013) P10016
[4] K. Aamodt *et al.* [ALICE Collaboration], JINST **5** (2010) P03003
[5] J. Alme *et al.*, Nucl. Instrum. Meth. A **622** (2010) 316
[6] A. Akindinov *et al.*, Eur. Phys. J. Plus **128** (2013) 44.
[7] M. L. Miller, K. Reygers, S. J. Sanders and P. Steinberg, Ann. Rev. Nucl. Part. Sci. **57** (2007) 205
[8] B. B. Abelev *et al.* [ALICE Collaboration], Phys. Lett. B **728** (2014) 216 Corrigendum: [Phys. Lett. B **734** (2014) 409]
[9] B. B. Abelev *et al.* [ALICE Collaboration], Phys. Lett. B **728** (2014) 25
[10] J. Adam *et al.* [ALICE Collaboration], Phys. Lett. B **758** (2016) 389
[11] J. Adam *et al.* [ALICE Collaboration], Phys. Rev. C **93** (2016) no.3, 034913
[12] B. B. Abelev *et al.* [ALICE Collaboration], Phys. Rev. Lett. **111** (2013) 222301
[13] J. Adam *et al.* [ALICE Collaboration], Phys. Lett. B **760** (2016) 720 doi:10.1016/j.physletb.2016.07.050 [arXiv:1601.03658 [nucl-ex]].
[14] B. Abelev *et al.* [ALICE Collaboration], Phys. Rev. Lett. **110** (2013) no.8, 082302
[15] B. Abelev *et al.* [ALICE Collaboration], Phys. Rev. C **88** (2013) 044910
[16] P. Skands, S. Carrazza and J. Rojo, Eur. Phys. J. C **74** (2014) no.8, 3024
[17] X. N. Wang and M. Gyulassy, Phys. Rev. D **44** (1991) 3501.
[18] R. Brun, F. Bruyant, F. Carminati, S. Giani, M. Maire, A. McPherson, G. Patrick and L. Urban, CERN-W5013.
[19] T. Pierog, I. Karpenko, J. M. Katzy, E. Yatsenko and K. Werner, Phys. Rev. C **92** (2015) no.3, 034906
[20] B. Abelev *et al.* [ALICE Collaboration], Phys. Lett. B **720** (2013) 52
[21] M. Djordjevic, B. Blagojevic and L. Zivkovic, Phys. Rev. C **94** (2016) no.4, 044908
[22] A. Majumder and C. Shen, Phys. Rev. Lett. **109** (2012) 202301
[23] Y. T. Chien, A. Emerman, Z. B. Kang, G. Ovanesyan and I. Vitev, Phys. Rev. D **93** (2016) no.7, 074030
[24] G. Ovanesyan and I. Vitev, Phys. Lett. B **706** (2012) 371